EARTHQUAKE ENGINEERING AND STRUCTURAL DYNAMICS
Earthquake Engng. Struct. Dyn. **28**, 1163–1185 (1999)

DYNAMIC CHARACTERISTICS AND SEISMIC RESPONSE OF ADJACENT BUILDINGS LINKED BY DISCRETE DAMPERS

W. S. ZHANG AND Y. L. XU*
Department of Civil and Structural Engineering, The Hong Kong Polytechnic University, Hung Hom, Kowloon, Hong Kong

SUMMARY

Coupling adjacent buildings using discrete viscoelastic dampers for control of response to low and moderate seismic events is investigated in this paper. The complex modal superposition method is first used to determine dynamic characteristics, mainly modal damping ratio and modal frequency, of damper-linked linear adjacent buildings for practical use. Random seismic response of linear adjacent buildings linked by dampers is then determined by a combination of the complex modal superposition method and the pseudo-excitation method. This combined method can effectively and accurately determine random seismic response of non-classically damped systems in the frequency domain. Parametric studies are finally performed to identify optimal parameters of viscoelastic dampers for achieving the maximum modal damping ratio or the maximum response reduction of adjacent buildings. It is demonstrated that using discrete viscoelastic dampers of proper parameters to link adjacent buildings can reduce random seismic responses significantly. Copyright © 1999 John Wiley & Sons Ltd.

KEY WORDS: adjacent buildings; discrete damper; modal damping ratio; seismic response; analytical method; parametric study

INTRODUCTION

Buildings in a modern city are often built closely to each other due to limited land available. These buildings, in most cases, are separated without any structural connections or are connected only at the ground level. Hence, earthquake-resistant capacity of each building mainly depends on itself. To improve the earthquake resistance of these buildings, the concept of using control devices to link adjacent buildings has been presented.

Kobori *et al.*[1] developed bell-shaped hollow connectors to link very closely spaced adjacent buildings in a complex. The bell-shaped hollow connector is made of steel with stabilized hysteretic characteristic when the connector yields so that it can absorb vibration energy from earthquake. However, the high stiffness of the connector may significantly change the dynamic characteristics of the original buildings. The yield strength of the connector is also difficult to decide because if the yield strength is too high, the connector may not function properly but if the yield strength is too low, the energy adsorbing capacity may be too small. Seto and Matsumoto[2]

* Correspondence to: Y. L. Xu, Department of Civil and Structural Engineering, The Hong Kong Polytechnic University, Hung Hom, Kowloon, Hong Kong

CCC 0098–8847/99/101163–23$17·50

Received 8 October 1998
Accepted 12 May 1999

suggested using active actuators to connect a group of buildings for controlling their seismic responses. Yamada *et al.*[3] let active actuators generate negative stiffness so as to shift the natural frequencies of adjacent buildings away from the dominant frequency of ground motion to reduce seismic responses. Though the idea of using active actuators is promising, some practical problems, such as spillover and power supply, have to be solved before it can be put into practice.

Xu and He[4] recently investigated earthquake resistant performance of adjacent buildings connected by viscoelastic dampers. The Voigt model[5] is employed to represent the viscoelastic dampers. Since adjacent buildings connected by discrete viscoelastic dampers form a non-classically damped system, a pseudo-excitation method was used in their study to determine random seismic response of the building–damper systems. The pseudo-excitation method they used, however, can not predict dynamic characteristics of the adjacent building–damper system so that the practical response spectrum method stipulated in most of the seismic design codes can not be applied to this case. In addition, the pseudo-excitation method in conjunction with modal reduction technique can provide only an approximate solution to non-classically damped systems.

The objectives of this study are thus (1) to determine dynamic characteristics of adjacent buildings linked by viscoelastic dampers represented by the Voigt model; (2) to find an efficient and accurate method for determining random seismic response of non-classically damped systems; and (3) to identify optimal parameters of viscoelastic dampers for achieving the maximum modal damping ratio or the maximum seismic response reduction of adjacent buildings.

There have been many studies with the objective for providing computationally efficient modal solution techniques to determine random seismic response of non-classically damped systems. Singh[6] simplified the complex modal superposition method to the complex SRSS (square root of the sum of the squares of response variables) method for non-classically damped systems subject to seismic excitation. Igusa *et al.*[7] used the complex mode superposition method for evaluating the spectral moments of response. Veletsos and Ventura[8] expressed the displacement responses of a non-classically damped n-degree-of-freedom system as a linear combination of the displacement and velocity responses of n similarly excited single-degree-of-freedom systems in the time domain. An iterative procedure was presented by Claret and Venancio[9] for determining the response of the system to specified time history.

In the present study, the complex mode superposition method is used for investigating dynamic characteristics of viscoelastic damper-connected linear adjacent buildings. A combination of the complex mode superposition method and the pseudo-excitation method is proposed to efficiently and accurately determine random seismic response of linear adjacent buildings with discrete dampers. Optimal parameters of viscoelastic dampers for achieving the maximum seismic response reduction of adjacent buildings are identified through both parametric and sensitivity studies.

MODELLING OF THE SYSTEM

To capture important characteristics of damper-connected adjacent buildings and to make the problem manageable, only the two-dimensional system consisting of two linear elastic shear buildings connected by viscoelastic dampers at each floor of the same level is considered in the present study (see Figure 1). The assumption of linear elastic buildings indicates that only small

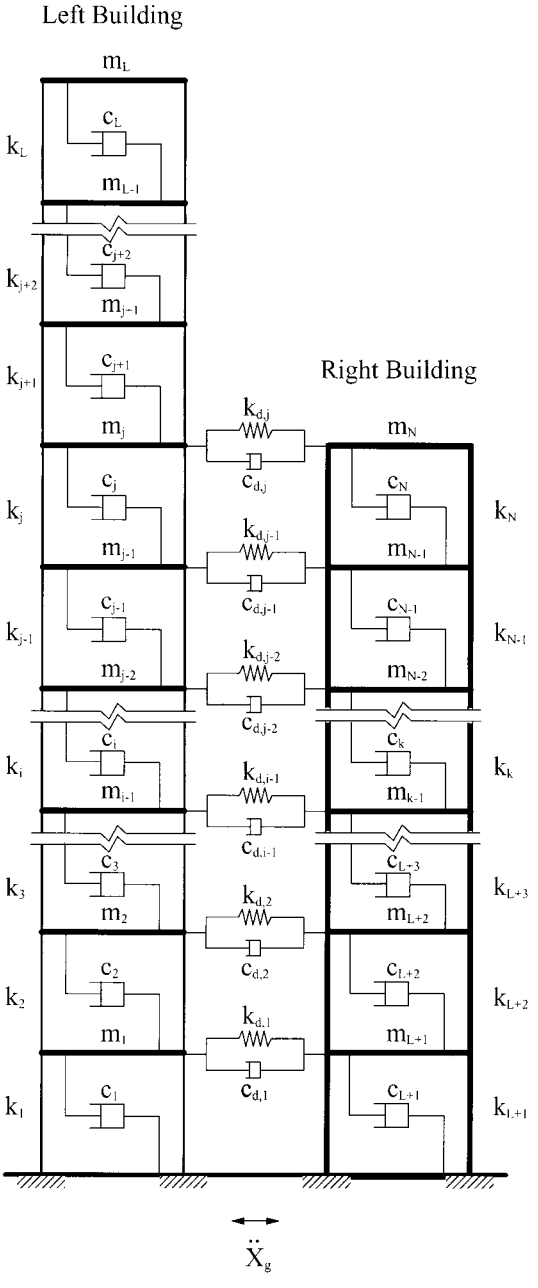

Figure 1. Structural model of adjacent buildings with joint dampers

and moderate seismic events are concerned. Each viscoelastic damper is represented by the Voigt model; that is, a linear and elastic spring and a viscous dashpot are combined in parallel. The mass of each building is concentrated at its floor and the stiffness is provided by its massless columns. Both buildings are assumed to be subject to the same base acceleration and any

effects due to spatial variations of the ground motion or due to soil-structure interactions are neglected.

Assume that a total degrees of freedom of two adjacent buildings are N (see Figure 1), in which the number of degrees of freedom of the left building is L with its first floor designated as the first degree of freedom. $N - L$ is then the number of degrees of freedom of the right building with its first floor designated as the $L + 1$ degree of freedom. The equations of motion of the building-damper system can be expressed as

$$\mathbf{M}\ddot{\mathbf{X}}(t) + \mathbf{C}\dot{\mathbf{X}}(t) + \mathbf{K}\mathbf{X}(t) = -\mathbf{M}\mathbf{E}\ddot{X}_{\mathrm{g}}(t) \tag{1}$$

where $\mathbf{M}$ is the mass matrix of the adjacent buildings; $\mathbf{K}$ and $\mathbf{C}$ are the total stiffness and damping matrices of the system, respectively, including structural stiffness and damping coefficients as well as the stiffness and damping coefficients from viscoelastic dampers; $\mathbf{X}(t)$ is the vector of relative displacement response with respect to the ground with the left building's displacements in the first L positions and the right building's displacement in the last $N - L$ positions; $\mathbf{E}$ is the index vector with all its elements equal to 1; and $\ddot{X}_{\mathrm{g}}(t)$ is the ground acceleration.

Denote the mass, shear stiffness, and external damping coefficient and internal damping coefficient of the adjacent buildings as m_i, k_i, b_i, c_i $(i = 1, 2, \ldots, N)$, respectively, and the damping coefficient and stiffness coefficient of the viscoelastic damper at the ith floor as $c_{\mathrm{d}i}$ and $k_{\mathrm{d}i}$, respectively. The details of each matrix in equation (1) can be then given as follows:

$$\mathbf{M} = \mathrm{diag}[m_1, m_2, \ldots, m_N] \tag{2}$$

$$\mathbf{C} = \mathbf{C}^{\mathrm{e}} + \mathbf{C}^{\mathrm{i}} + \mathbf{C}^{\mathrm{d}} \tag{3}$$

$$\mathbf{K} = \mathbf{K}^{\mathrm{s}} + \mathbf{K}^{\mathrm{d}} \tag{4}$$

in which the external damping matrix is

$$\mathbf{C}^{\mathrm{e}} = \mathrm{diag}[b_1, b_2, \ldots, b_N] \tag{5}$$

The internal damping matrix is

$$\mathbf{C}^{\mathrm{i}} = \begin{bmatrix} \mathbf{C}_L & \mathbf{0} \\ \mathbf{0} & \mathbf{C}_{\mathrm{R}} \end{bmatrix} \tag{6}$$

$$\mathbf{C}_{\mathrm{L}} = \begin{bmatrix} c_1 + c_2 & -c_2 & & & & \\ -c_2 & c_2 + c_3 & \ddots & & & \\ & & & -c_{L-1} & c_{L-1} + c_L & -c_L \\ & & & & -c_L & c_L \end{bmatrix} \tag{7}$$

$$\mathbf{C}_{\mathrm{R}} = \begin{bmatrix} c_{L+1} + c_{L+2} & -c_{L+2} & & & & \\ -c_{L+2} & c_{L+2} + c_{L+3} & \ddots & & & \\ & & & -c_{N-1} & c_{N-1} + c_N & -c_N \\ & & & & -c_N & c_N \end{bmatrix} \tag{8}$$

The damping matrix attributed to the viscoelastic dampers is

$$\mathbf{C}^{\mathrm{d}} = \begin{bmatrix} \mathbf{C}_{(N-L)\times(N-L)} & \mathbf{0}_{(N-L)\times(2L-N)} & -\mathbf{C}_{(N-L)\times(N-L)} \\ \mathbf{0}_{(2L-N)\times(N-L)} & \mathbf{0}_{(2L-N)\times(2L-N)} & \mathbf{0}_{(2L-N)\times(N-L)} \\ -\mathbf{C}_{(N-L)\times(N-L)} & \mathbf{0}_{(N-L)\times(2L-N)} & \mathbf{C}_{(N-L)\times(N-L)} \end{bmatrix} \quad (\text{if } N < 2L) \tag{9}$$

$$\mathbf{C}_{(N-L)\times(N-L)} = \mathrm{diag}[c_{\mathrm{d}1}, c_{\mathrm{d}2}, \ldots, c_{\mathrm{d}N-L}] \tag{10}$$

or

$$\mathbf{C}^{\mathrm{d}} = \begin{bmatrix} \mathbf{C}_{L\times L} & -\mathbf{C}_{L\times L} & \mathbf{0}_{L\times(N-2L)} \\ -\mathbf{C}_{L\times L} & \mathbf{C}_{L\times L} & \mathbf{0}_{L\times(N-2L)} \\ \mathbf{0}_{(N-2L)\times L} & \mathbf{0}_{(N-2L)\times L} & \mathbf{0}_{(N-2L)\times(N-2L)} \end{bmatrix} \quad (\text{if } N \geqslant 2L) \tag{11}$$

$$\mathbf{C}_{L\times L} = \mathrm{diag}[c_{\mathrm{d}1}, c_{\mathrm{d}2}, \ldots, c_{\mathrm{d}L}] \tag{12}$$

The stiffness matrix of the adjacent buildings is

$$\mathbf{K}^{\mathrm{s}} = \begin{bmatrix} \mathbf{K}_L & \mathbf{0} \\ \mathbf{0} & \mathbf{K}_R \end{bmatrix} \tag{13}$$

$$\mathbf{K}_L = \begin{bmatrix} k_1 + k_2 & -k_2 & & & & \\ -k_2 & k_2 + k_3 & & & & \\ & & \ddots & & & \\ & & & \ddots & & \\ & & & -k_{L-1} & k_{L-1} + k_L & -k_L \\ & & & & -k_L & k_L \end{bmatrix} \tag{14}$$

$$\mathbf{K}_R = \begin{bmatrix} k_{L+1} + k_{L+2} & -k_{L+2} & & & & \\ -k_{L+2} & k_{L+2} + k_{L+3} & & & & \\ & & \ddots & & & \\ & & & \ddots & & \\ & & & -k_{N-1} & k_{N-1} + k_N & -k_N \\ & & & & -k_N & k_N \end{bmatrix} \tag{15}$$

The stiffness matrix attributed to the viscoelastic dampers is

$$\mathbf{K}^{\mathrm{d}} = \begin{bmatrix} \mathbf{K}_{(N-L)\times(N-L)} & \mathbf{0}_{(N-L)\times(2L-N)} & -\mathbf{K}_{(N-L)\times(N-L)} \\ \mathbf{0}_{(2L-N)\times(N-L)} & \mathbf{0}_{(2L-N)\times(2L-N)} & \mathbf{0}_{(2L-N)\times(N-L)} \\ -\mathbf{K}_{(N-L)\times(N-L)} & \mathbf{0}_{(N-L)\times(2L-N)} & \mathbf{K}_{(N-L)\times(N-L)} \end{bmatrix} \quad (\text{if } N < 2L) \tag{16}$$

$$\mathbf{K}_{(N-L)\times(N-L)} = \mathrm{diag}[k_{\mathrm{d}1}, k_{\mathrm{d}2}, \ldots, k_{\mathrm{d}N-L}] \tag{17}$$

or

$$\mathbf{K}^{\mathrm{d}} = \begin{bmatrix} \mathbf{K}_{L\times L} & -\mathbf{K}_{L\times L} & \mathbf{0}_{L\times(N-2L)} \\ -\mathbf{K}_{L\times L} & \mathbf{K}_{L\times L} & \mathbf{0}_{L\times(N-2L)} \\ \mathbf{0}_{(N-2L)\times L} & \mathbf{0}_{(N-2L)\times L} & \mathbf{0}_{(N-2L)\times(N-2L)} \end{bmatrix} \quad (\text{if } N \geqslant 2L) \tag{18}$$

$$\mathbf{K}_{L\times L} = \mathrm{diag}[k_{\mathrm{d}1}, k_{\mathrm{d}2}, \ldots, k_{\mathrm{d}L}] \tag{19}$$

SOLUTION FOR DYNAMIC CHARACTERISTICS

The application of the response spectrum analysis method requires estimates of the dynamic characteristics of the system to be available. Since the adjacent buildings linked by viscoelastic dampers are non-classically damped systems, to facilitate the seismic design of such systems the complex mode superposition method[10] is employed in this study to estimate their dynamic characteristics.

For the homogeneous form of equation (1), a general solution can be assumed of the form

$$\mathbf{X}(t) = \boldsymbol{\phi}\mathrm{e}^{st} \tag{20}$$

in which s is the eigenvalue and $\boldsymbol{\phi}$ is the associated eigenvector. Equation (1) can be also reformulated into a first-order $2N$-dimensional equation

$$\mathbf{A}\dot{\mathbf{Y}} + \mathbf{B}\mathbf{Y} = \mathbf{F}\ddot{X}_{\mathrm{g}}(t) \tag{21}$$

where

$$\mathbf{A} = \begin{bmatrix} \mathbf{0} & \mathbf{M} \\ \mathbf{M} & \mathbf{C} \end{bmatrix}, \quad \mathbf{B} = \begin{bmatrix} -\mathbf{M} & \mathbf{0} \\ \mathbf{0} & \mathbf{K} \end{bmatrix}, \quad \mathbf{F} = \begin{Bmatrix} \mathbf{0} \\ -\mathbf{ME} \end{Bmatrix} \quad \text{and} \quad \mathbf{Y} = \begin{Bmatrix} \dot{\mathbf{X}} \\ \mathbf{X} \end{Bmatrix} \tag{22}$$

The solution of the homogeneous form of equation (21) can be then taken as

$$\mathbf{Y} = \begin{Bmatrix} s\boldsymbol{\phi} \\ \boldsymbol{\phi} \end{Bmatrix} \mathrm{e}^{st} = \hat{\boldsymbol{\phi}}\mathrm{e}^{st} \tag{23}$$

The associated eigenvalue problem of equation (21) becomes

$$(s\mathbf{A} + \mathbf{B})\hat{\boldsymbol{\phi}} = \mathbf{0} \tag{24}$$

Underdamped system

The solution of equation (24) comprises a set of $2N$ eigenvalues and eigenvectors that are real or exist in complex conjugate pairs. If all the eigenvalues and eigenvectors are in complex conjugate pairs with negative real parts, the system is defined as the underdamped system. For a underdamped system,

$$\hat{\boldsymbol{\phi}}_j = \hat{\boldsymbol{\phi}}^*_{j+N} \quad \text{and} \quad s_j = s^*_{j+N} \quad (j = 1, 2, \ldots, N) \tag{25}$$

Each eigenvalue is usually written under the form

$$s_j = s^*_{j+N} = -\omega_j\xi_j + \mathrm{i}\omega_{\mathrm{d}j}\,(j = 1, 2, \ldots, N) \tag{26}$$

in which

$$\omega_j = |s_j|, \quad \xi_j = -\operatorname{Re}(s_j)/|s_j| \quad \text{and} \quad \omega_{dj} = \omega_j\sqrt{1-\xi_j^2} \tag{27}$$

ω_j, ω_{dj}, and ξ_j are the modal frequency, the damped modal frequency, and the modal damping ratio, respectively, associated with mode j. The superscript* means the conjugation. For the underdamped system, the value of ξ_j is always less than one.

To find the sensitivity of modal frequency and modal damping ratio to the damping coefficient c_{dm} of the mth damper, the partial derivative of equation (24) with respect to c_{dm}, is taken.

$$\left(\frac{\partial s_j}{\partial c_{dm}}\mathbf{A} + s_j\frac{\partial \mathbf{A}}{\partial c_{dm}}\right)\hat{\boldsymbol{\phi}}_j + (s_j\mathbf{A}+\mathbf{B})\frac{\partial \hat{\boldsymbol{\phi}}_j}{\partial c_{dm}} = \mathbf{0} \tag{28}$$

Since the matrices A and B are symmetric, the following relationship exists by means of equation (24):

$$\hat{\boldsymbol{\phi}}_j^{\mathrm{T}}(s_j\mathbf{A}+\mathbf{B}) = \mathbf{0} \tag{29}$$

Multiplying equation (28) by $\hat{\boldsymbol{\phi}}_j^{\mathrm{T}}$ and using equation (29) lead to

$$\frac{\partial s_j}{\partial c_{dm}} = -\left(s_j\hat{\boldsymbol{\phi}}_j^{\mathrm{T}}\frac{\partial \mathbf{A}}{\partial c_{dm}}\hat{\boldsymbol{\phi}}_j\right)\Big/ A_j = -s_jC_{jm}/A_j \tag{30}$$

in which

$$C_{jm} = \hat{\boldsymbol{\phi}}_j^{\mathrm{T}}\frac{\partial \mathbf{A}}{\partial c_{dm}}\hat{\boldsymbol{\phi}}_j = \hat{\boldsymbol{\phi}}_j^{\mathrm{T}}\frac{\partial \mathbf{C}}{\partial c_{dm}}\boldsymbol{\phi}_j \tag{31}$$

$$A_j = \hat{\boldsymbol{\phi}}_j^{\mathrm{T}}\mathbf{A}\hat{\boldsymbol{\phi}}_j \tag{32}$$

For the underdamped system, differentiating the following relationships with respect to the mth damper damping coefficient c_{dm}

$$s_js_j^* = \omega_j^2 \quad \text{and} \quad s_j + s_j^* = -2\xi_j\omega_j \tag{33}$$

and using equation (30) yield

$$\frac{\partial \omega_j}{\partial c_{dm}} = -\omega_j\operatorname{Re}\left(\frac{C_{jm}}{A_j}\right) \tag{34}$$

$$\frac{\partial \xi_j}{\partial c_{dm}} = -\sqrt{1-\xi_j^2}\operatorname{Im}\left(\frac{C_{jm}}{A_j}\right) \tag{35}$$

By using equations (34) and (35), the sensitivity of jth modal frequency and jth modal damping ratio to the damping coefficient c_{dm} of the mth damper can be found. In a similar way, the sensitivity of jth modal frequency and jth modal damping ratio to the stiffness coefficient k_{dm} of the mth damper can be obtained.

$$\frac{\partial \omega_j}{\partial k_{dm}} = \xi_j\operatorname{Re}\left(\frac{K_{jm}}{A_j}\right) - \sqrt{1-\xi_j^2}\operatorname{Im}\left(\frac{K_{jm}}{A_j}\right) \tag{36}$$

$$\frac{\partial \xi_j}{\partial k_{dm}} = \frac{\sqrt{1-\xi_j^2}}{\omega_j}\left[\xi_j\operatorname{Im}\left(\frac{K_{jm}}{A_j}\right) + \sqrt{1-\xi_j^2}\operatorname{Re}\left(\frac{K_{jm}}{A_j}\right)\right] \tag{37}$$

in which

$$K_{jm} = \boldsymbol{\phi}_j^{\mathrm{T}} \frac{\partial \mathbf{K}}{\partial k_{\mathrm{d}m}} \boldsymbol{\phi}_j \tag{38}$$

System with mixed damping

For the adjacent buildings connected by viscoelastic dampers, equation (24) may produce some real-valued negative pairs, each associated with a real-valued eigenvector, in addition to some eigenvalues and eigenvectors which are in complex conjugate pairs with negative real parts. In this case, the system may be called the mixed damped system in general, and it is convenient to express real pairs s_j in the following form analogous to equation (26).

$$s_j = -\omega_j \xi_j + \omega_{\mathrm{d}j} \quad (j = 1, 2, \ldots, N) \tag{39}$$

$$s_{j+N} = -\omega_j \xi_j - \omega_{\mathrm{d}j} \quad (j = 1, 2, \ldots, N) \tag{40}$$

in which ω_j, $\omega_{\mathrm{d}j}$ and ξ_j are determined by

$$\omega_j = \sqrt{s_j s_{j+N}}, \quad \xi_j = -(s_j + s_{j+N})/(2\omega_j) \quad \text{and} \quad \omega_{\mathrm{d}j} = \omega_j \sqrt{\xi_j^2 - 1} = (s_j - s_{j+N})/2 \tag{41}$$

The value of ξ_j is now equal to or greater than one. The sensitivity study of the modal frequency and modal damping ratio with respect to the mth damper damping coefficient $c_{\mathrm{d}m}$ or the mth damper stiffness coefficient $k_{\mathrm{d}m}$ is based on the following equations:

$$\frac{\partial \omega_j}{\partial c_{\mathrm{d}m}} = -\frac{\omega_j}{2}\left(\frac{C_{jm}}{A_j} + \frac{C_{j+N,m}}{A_{j+N}}\right) \tag{42}$$

$$\frac{\partial \xi_j}{\partial c_{\mathrm{d}m}} = \frac{\sqrt{\xi_j^2 - 1}}{2}\left(\frac{C_{jm}}{A_j} - \frac{C_{j+N,m}}{A_{j+N}}\right) \tag{43}$$

$$\frac{\partial \omega_j}{\partial k_{\mathrm{d}m}} = \frac{\xi_j}{2}\left(\frac{K_{j,m}}{A_j} + \frac{K_{j+N,m}}{A_{j+N}}\right) + \frac{\sqrt{\xi_j^2 - 1}}{2}\left(\frac{K_{j,m}}{A_j} - \frac{K_{j+N,m}}{A_{j+N}}\right) \tag{44}$$

$$\frac{\partial \xi_j}{\partial k_{\mathrm{d}m}} = -\frac{\sqrt{\xi_j^2 - 1}}{2\omega_j}\left[\sqrt{\xi_j^2 - 1}\left(\frac{K_{j,m}}{A_j} + \frac{K_{j+N,m}}{A_{j+N}}\right) + \xi_j\left(\frac{K_{j,m}}{A_j} - \frac{K_{j+N,m}}{A_{j+N}}\right)\right] \tag{45}$$

SOLUTION FOR SEISMIC RESPONSE

The complex mode superposition method adopts the following co-ordinate transformation to decouple equation (21)

$$\mathbf{Y} = \Phi \mathbf{Z} \tag{46}$$

where $\mathbf{Z}$ is the $2N$-dimensional generalized coordinate vector and Φ is the $2N \times 2N$ complex modal matrix

$$\Phi = [\hat{\boldsymbol{\phi}}_1, \hat{\boldsymbol{\phi}}_2, \ldots, \hat{\boldsymbol{\phi}}_{2N}] \tag{47}$$

By using the co-ordinate transformation and the orthogonality of modes, equation (21) can be reduced to $2N$ decoupled modal equations with the jth modal equation being

$$A_j\dot{Z}_j + B_jZ_j = \hat{\boldsymbol{\phi}}_j^{\mathrm{T}}\mathbf{F}\ddot{X}_{\mathrm{g}}(t) \tag{48}$$

or alternatively

$$\dot{Z}_j - s_jZ_j = r_j\ddot{X}_g(t) \tag{49}$$

in which

$$B_j = \hat{\boldsymbol{\phi}}_j^{\mathrm{T}}\mathbf{B}\hat{\boldsymbol{\phi}}_j = -s_jA_j \tag{50}$$

$$r_j = \hat{\boldsymbol{\phi}}_j^{\mathrm{T}}\mathbf{F}/A_j = -\boldsymbol{\phi}_j^{\mathrm{T}}\mathbf{ME}/A_j \tag{51}$$

Assume that the ground acceleration $\ddot{X}_{\mathrm{g}}(t)$ is a stationary random process and its power spectral density function is given as $S_{\mathrm{g}}(\omega)$. A pseudo-excitation method in conjunction with the complex mode superposition method are now developed to determine the seismic response of adjacent buildings connected by viscoelastic dampers.

The pseudo-excitation is constituted for a given frequency ω as

$$\ddot{X}_{\mathrm{g}}(t) = \sqrt{S_{\mathrm{g}}(\omega)}\,\mathrm{e}^{\mathrm{i}\omega t} \tag{52}$$

The solution of the first-order equation (49) to the pseudo-excitation is

$$Z_j(\omega, t) = \frac{r_j}{\mathrm{i}\omega - s_j}\sqrt{S_{\mathrm{g}}(\omega)}\,\mathrm{e}^{\mathrm{i}\omega t} \quad (j = 1, 2, \ldots, 2N) \tag{53}$$

Substituting equation (53) into equation (46) and comparing with the last part of equation (22), one obtains

$$\mathbf{X}(\omega, t) = \sum_{j=1}^{2N}\boldsymbol{\phi}_jZ_j(\omega, t) = \sum_{j=1}^{2N}\boldsymbol{\phi}_j\frac{r_j}{\mathrm{i}\omega - s_j}\sqrt{S_{\mathrm{g}}(\omega)}\,\mathrm{e}^{\mathrm{i}\omega t} \tag{54}$$

Since the eigenvector is in pairs in either underdamped system or the system with mixed damping, the $\mathbf{X}(\omega, t)$ can be reduced to

$$\mathbf{X}(\omega, t) = \sum_{j=1}^{N}H_j(\omega)(\mathrm{i}\omega\boldsymbol{\alpha}_j + \boldsymbol{\beta}_j)\sqrt{S_{\mathrm{g}}(\omega)}\,\mathrm{e}^{\mathrm{i}\omega t} = \mathbf{X}(\omega)\,\mathrm{e}^{\mathrm{i}\omega t} \tag{55}$$

in which $\mathbf{X}(\omega)$ is called pseudo-displacement

$$\mathbf{X}(\omega) = \sum_{j=1}^{N}H_j(\omega)(\mathrm{i}\omega\boldsymbol{\alpha}_j + \boldsymbol{\beta}_j)\sqrt{S_{\mathrm{g}}(\omega)} \tag{56}$$

$H_j(\omega)$ is the frequency response function for the jth mode.

$$H_j(\omega) = \frac{1}{\omega_j^2 - \omega^2 + \mathrm{i}2\xi_j\omega_j\omega} \tag{57}$$

When the jth mode is a underdamped mode,

$$\boldsymbol{\alpha}_j = 2\,\mathrm{Re}(\boldsymbol{\phi}_jr_j) \quad \text{and} \quad \boldsymbol{\beta}_j = -2\,\mathrm{Re}(\boldsymbol{\phi}_jr_js_j^*) \tag{58}$$

When the jth mode is an overdamped mode or a critically damped case

$$\boldsymbol{\alpha}_j = (\boldsymbol{\phi}_j r_j + \boldsymbol{\phi}_{j+N} r_{j+N}) \quad \text{and} \quad \boldsymbol{\beta}_j \sim -(\boldsymbol{\phi}_j r_j s_{j+N} + \boldsymbol{\phi}_{j+N} r_{j+N} s_j) \tag{59}$$

Similarly, the pseudo-velocity response can be obtained by

$$\dot{\mathbf{X}}(\omega) = \sum_{j=1}^{N} H_j(\omega)(\mathrm{i}\omega\boldsymbol{\mu}_j \to \boldsymbol{\nu}_j)\sqrt{S_{\mathrm{g}}(\omega)} \tag{60}$$

in which when the jth mode is a underdamped mode

$$\boldsymbol{\mu}_j = 2\,\mathrm{Re}(s_j \boldsymbol{\phi}_j r_j) \text{ and } \boldsymbol{\nu}_j = -2\omega_j^2\,\mathrm{Re}(\boldsymbol{\phi}_j r_j) \tag{61}$$

When the jth mode is an overdamped mode or a critically damped case

$$\boldsymbol{\mu}_j \sim (s_j \boldsymbol{\phi}_j r_j + s_{j+N} \boldsymbol{\phi}_{j+N} r_{j+N}) \quad \text{and} \quad \boldsymbol{\nu}_j = -\omega_j^2(\boldsymbol{\phi}_j r_j + \boldsymbol{\phi}_{j+N} r_{j+N}) \tag{62}$$

Once the pseudo-displacement is determined, the pseudo-internal force can be easily determined following a static analysis. For instance, the pseudo-shear force of the adjacent buildings can be calculated by

$$\mathbf{Q}(\omega, t) = \mathbf{G}\mathbf{X}(\omega, t) \tag{63}$$

where

$$\mathbf{G} = \begin{bmatrix} \mathbf{G}_L & 0 \\ 0 & \mathbf{G}_R \end{bmatrix} \tag{64}$$

and

$$\mathbf{G}_L = \begin{bmatrix} k_1 & & & & & \\ -k_2 & k_2 & & & & \\ & \cdot & & & & \\ & & \cdot & & & \\ & & & -k_{L-1} & k_{L-1} & \\ & & & & -k_L & k_L \end{bmatrix} \tag{65}$$

$$\mathbf{G}_R = \begin{bmatrix} k_{L+1} & & & & & \\ -k_{L+2} & k_{L+2} & & & & \\ & \cdot & & & & \\ & & \cdot & & & \\ & & & -k_{N-1} & k_{N-1} & \\ & & & & -k_N & k_N \end{bmatrix} \tag{66}$$

The response spectral matrix can be then obtained by

$$\mathbf{S}_{xx}(\omega) = \mathbf{X}^*(\omega)\mathbf{X}^{\mathrm{T}}(\omega), \qquad \mathbf{S}_{x\dot{x}}(\omega) = \mathbf{X}^*(\omega)\dot{\mathbf{X}}^{\mathrm{T}}(\omega) \tag{67}$$

$$\mathbf{S}_{\dot{x}x}(\omega) = \dot{\mathbf{X}}^*(\omega)\mathbf{X}^{\mathrm{T}}(\omega), \quad \mathbf{S}_{\dot{x}\dot{x}}(\omega) = \dot{\mathbf{X}}^*(\omega)\dot{\mathbf{X}}^{\mathrm{T}}(\omega) \tag{68}$$

$$\mathbf{S}_{QQ}(\omega) = \mathbf{Q}^*(\omega)\mathbf{Q}^{\mathrm{T}}(\omega) \tag{69}$$

It should be pointed out that the pseudo-excitation method used in conjunction with complex mode superposition method is a natural extension of the original pseudo-excitation method suggested by Lin *et al.*[11] for the classically damped structures (or uncontrolled structures). By using the mixed method proposed here, the cross-correlation terms between vibration modes in the seismic response can be retained for the damper-connected adjacent buildings. The computational efforts for determining random seismic response is also reduced significantly, compared with the previous CQC (Complete Quadratic Combination) method.

The standard deviation displacement response of the jth floor σ_{x_j} is finally evaluated from $S_{x_j x_j}(\omega)$ through integration.

$$\sigma_{x_j}^2 = \int_{-\infty}^{+\infty} S_{x_j x_j}(\omega)\, \mathrm{d}\omega \tag{70}$$

The standard deviation acceleration response of the jth floor $\sigma_{\ddot{x}_j}$ is given by

$$\sigma_{\ddot{x}_j}^2 = \int_{-\infty}^{+\infty} \omega^2 S_{\dot{x}_j \dot{x}_j}(\omega)\, \mathrm{d}\omega \tag{71}$$

The Kanai–Tajimi filtered white noise spectrum is used as the ground acceleration spectrum in the computation in this study.

$$S_{\mathrm{g}}(\omega) = \frac{1 + 4\xi_{\mathrm{g}}^2(\omega/\omega_{\mathrm{g}})^2}{[1 - (\omega/\omega_{\mathrm{g}})^2]^2 + 4\xi_{\mathrm{g}}^2(\omega/\omega_{\mathrm{g}})^2}\, S_0 \tag{72}$$

in which ω_{g}, ξ_{g}, S_0 may be regarded as the characteristics and the intensity of an earthquake in a particular geological location.

APPLICATION TO EXAMPLE BUILDINGS

For application, two 20-storey buildings having the same floor elevations with dampers connecting two neighbouring floors are used. The mass, shear stiffness, and external damping coefficient of the left building (also called the stiffer building, see Figure 1) are uniform for all stories with the mass of $1{\cdot}29 \times 10^6$ kg, the shear stiffness of $4{\cdot}0 \times 10^9$ N/m, and the external damping coefficient of $1{\cdot}0 \times 10^5$ N s/m. For the right building (also called the softer building), the mass, shear stiffness, and external damping coefficient are also uniform for all stories with the same mass and damping coefficient as the left building but with the shear stiffness of $2{\cdot}0 \times 10^9$ N/m only. Hence, the two buildings have the same height but the natural frequencies are smaller in the right building than the left building. The internal damping coefficients are set to zero for both buildings. Viscoelastic dampers used to connect every two neighbouring floors are assumed to have the same damper damping coefficient and damper stiffness. The parameters in the ground acceleration spectrum are selected as $\omega_{\mathrm{g}} = 15{\cdot}0$ rad/s; $\xi_{\mathrm{g}} = 0{\cdot}65$ and $S_0 = 4{\cdot}65 \times 10^{-4}$ m^2/rad s^3.

Modal frequencies and modal damping ratios

The modal frequencies and damping ratios of each building without dampers-connected are calculated. Within the frequency range between zero and 21·00 rad/s, the first four modal frequencies of the right building are 3·02, 9·03, 14·99, and 20·87 rad/s, respectively. The first two modal frequencies of the left building are 4·27 and 12·77 rad/s, respectively. When every two neighbouring floors of the adjacent buildings are linked by the viscoelastic dampers of the same damping coefficient of $1{\cdot}0 \times 10^6$ N s/m and the same elastic stiffness of $1{\cdot}0 \times 10^5$ N/m, the first six modal frequencies of the damper-building system calculated by the complex mode superposition method are 3·14, 4·12, 9·07, 12·73, 15·02, and 20·88 rad/s, respectively. Clearly, using the viscoelastic dampers to link the adjacent buildings only slightly changes the modal frequencies of the individual building. The retention of the natural frequencies of the unlinked buildings after the installation of the joint dampers is especially desirable for the adjacent buildings that have been already built and need to be strengthened. As to modal damping ratios, the first four modal damping ratios in the unlinked left building are calculated as 1·28, 0·43, 0·26, and 0·19 per cent, respectively. The first two modal damping ratios in the unlinked right building are computed as 0·91 and 0·30 per cent, respectively. For the linked building–damper system, the first six modal damping ratios calculated by the complex mode superposition method

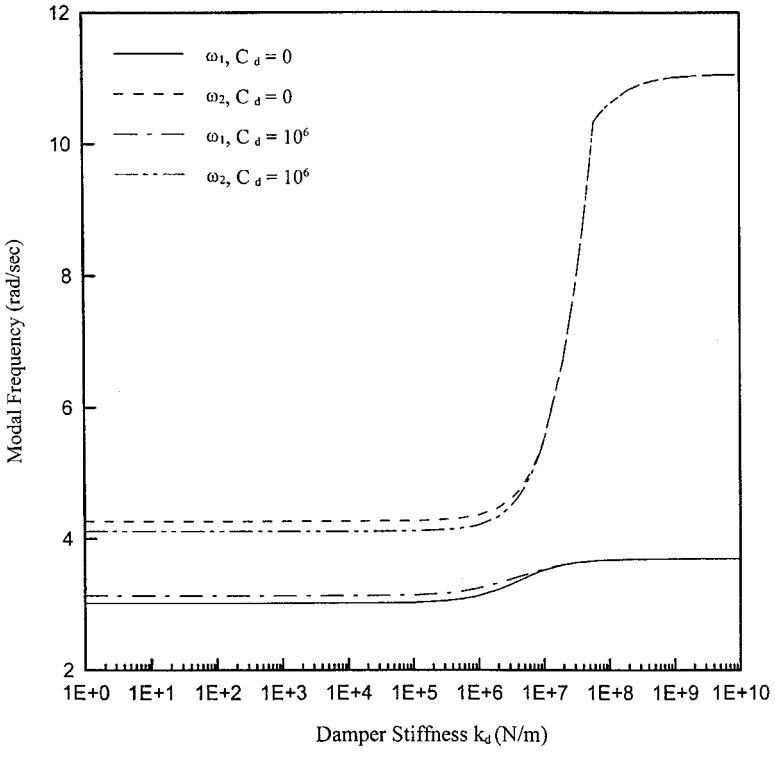

Figure 2. Variations of modal frequencies with damper stiffness

are 14·44, 9·68, 4·73, 3·33, 2·85 and 2·04 per cent, respectively. Obviously, the viscoelastic dampers offer significant damping to the adjacent buildings. Thus, one can expect that the seismic response of the adjacent buildings will be tremendously reduced.

The parameters used in the foregoing dampers are determined through a parametric study. In the parametric study, the modal frequencies and damping ratios of the building–damper system are computed against the stiffness and damping coefficient of the dampers. The beneficial stiffness k_d and damping coefficient c_d of the dampers can be thus found for achieving the maximum modal damping ratio and remaining the original modal frequencies unchanged. Figure 2 displays variations of the first- and second-modal frequencies of the system with damper stiffness k_d for damper damping coefficient $c_d = 0$ Ns/m and $c_d = 10^6$ Ns/m. It is seen that the modal frequencies are almost independent of damper stiffness when the damper stiffness is less than 5×10^5 N/m. However, if the damper stiffness is beyond this value, the second modal frequency of the system will have a rapid increase while the first modal frequency increases moderately. It is also seen from Figure 2 that the modal frequencies may not be sensitive to damper damping coefficient c_d, particularly in the case of the use of high damper stiffness. Figure 3 shows variations of the first two modal damping ratios of the system with damper stiffness for three damper damping coefficients. Clearly, the first two modal damping ratios of the system remain almost constant within a damper stiffness range from zero to 1×10^5 N/m. After this range, the first modal damping ratio will decrease rapidly with the increasing damper stiffness and the second modal

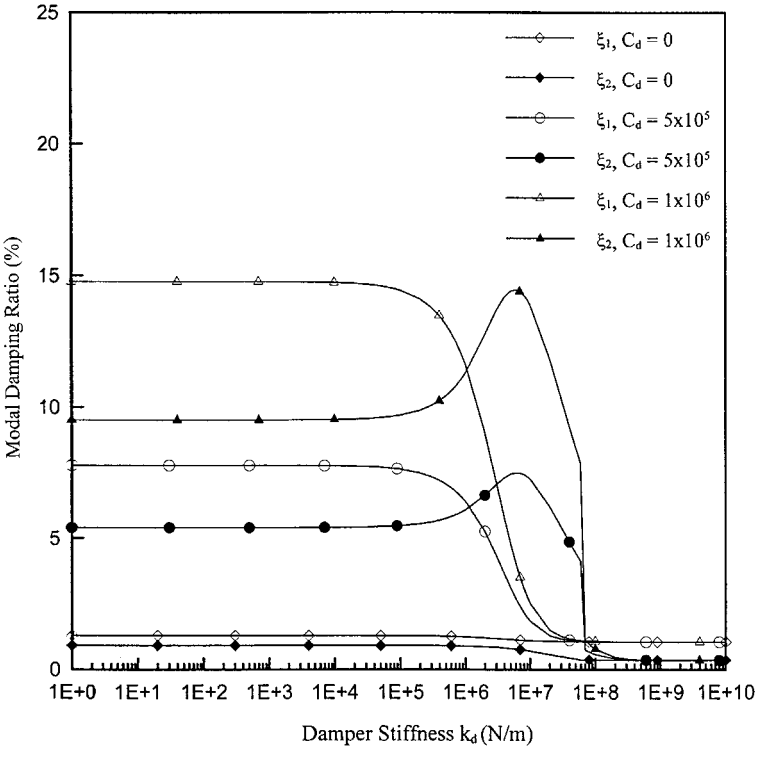

Figure. 3. Variations of modal damping ratios with damper stiffness

damping ratio will increase first and then decrease for the cases of non-zero damper damping coefficient. Thus, the optimal value of damper stiffness is selected as 1×10^5 N/m. Figure 3 also indicates that the damper damping coefficient affects the first two modal damping ratios of the system significantly.

The variations of the first six modal frequencies with damper damping coefficient are shown in Figure 4 for the damper stiffness of 1×10^5 N/m. All the modal frequencies remain almost constant when the damper damping coefficient is less than 1×10^6 Ns/m. After that, the modal frequencies have a sudden change: the four modal frequencies dominated by the softer building ($\omega_1, \omega_3, \omega_5$ and ω_6) become larger while the two modal frequencies governed by the stiffer building (ω_2 and ω_4) become smaller. This is an expected result for the dampers of very high damping coefficient. The modal damping ratios in the four modes dominated by the softer building (ξ_1, ξ_3, ξ_5 and ξ_6) are depicted in Figure 5(a) against the damper damping coefficient while the modal damping ratios in the two modes dominated by the stiffer building (ξ_2 and ξ_4) are plotted in Figure 5(b). It is seen that for the damper damping coefficient less than about 1×10^4 Ns/m, the dampers have no effect on the modal damping ratios, and the modal damping ratios come mainly from the buildings themselves. As the damper damping coefficient increases, all the modal damping ratios increase. However, when the damper damping coefficient is increased to certain values, the modal damping ratios dominated by the stiffer building decrease while the modal damping ratios governed by the softer building still increase and soon these

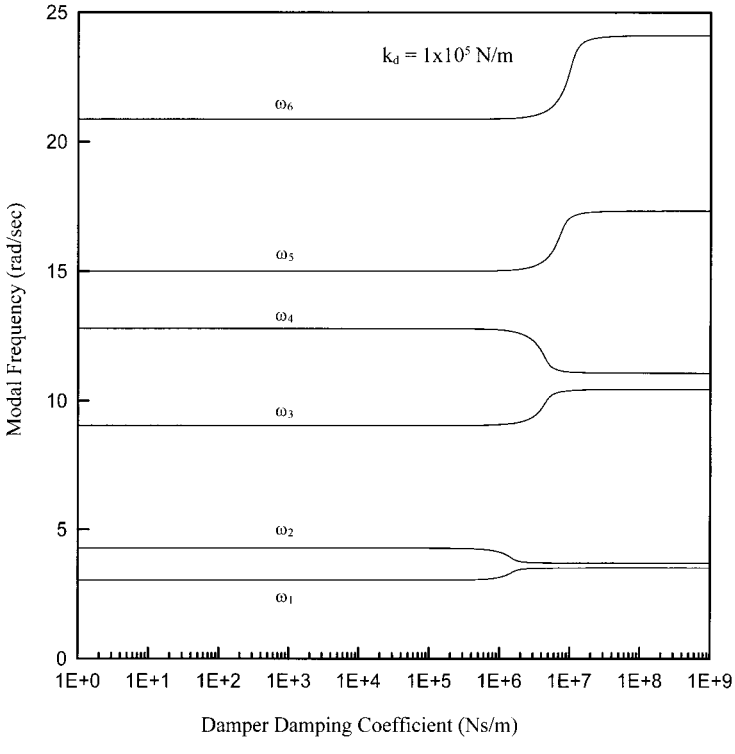

Figure. 4. Variations of modal frequencies with damper damping coefficient

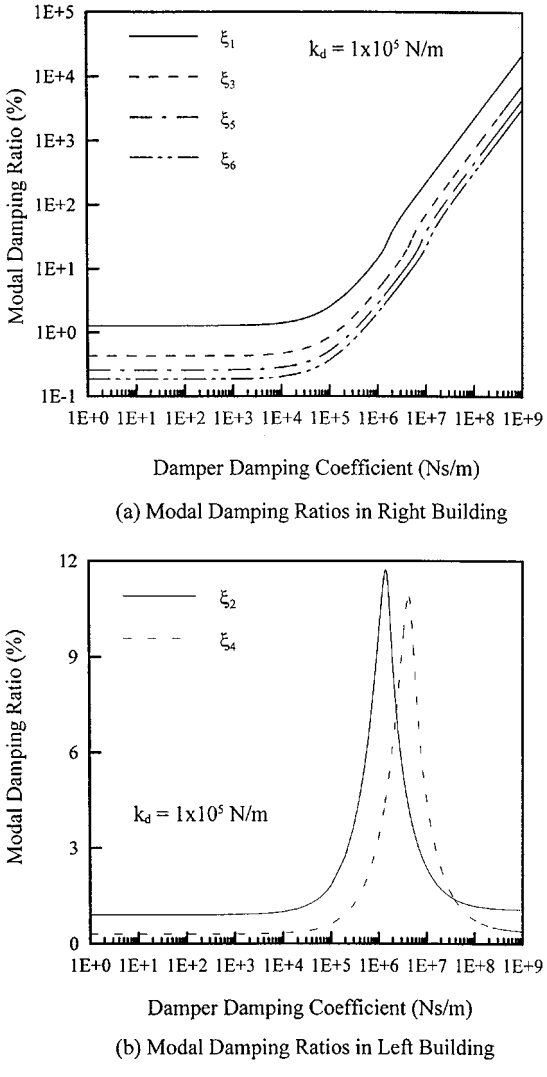

Figure. 5. Variations of modal damping ratios with damper damping coefficient

modes of the softer building become overdamped modes. Therefore, for a very large damper damping coefficient, the system behaves like a lightly damped stiffer building supported by a softer building almost without motion due to very high vibration energy dissipation capability. From a practical point of view, the optimum value of the damper damping coefficient should be selected around 1×10^6 Ns/m, by which all the modal damping ratios of either the stiffer building or the softer building reach certain values enough to reduce the seismic modal response of the whole system.

A sensitivity study of the modal frequency and modal damping ratio to damper stiffness and damper damping coefficient is carried out at the optimum values $c_d = 1 \times 10^6$ Ns/m

and $k_d = 1 \times 10^5$ N/m. The sensitivities of the first modal frequency ω_1 to changes in c_{di} or k_{di} $(i = 1, 2, \ldots, 20)$ are depicted in Figure 6(a) in terms of $\partial\omega_1/\partial c_{di}$ and $\partial\omega_1/\partial k_{di}$. The sensitivities of the first modal damping ratio ξ_1 to changes in c_{di} or k_{di} $(i = 1, 2, \ldots, 20)$ are plotted in Figure 6(b) by means of $\partial\xi_1/\partial c_{di}$ and $\partial\xi_1/\partial k_{di}$. As expected, the first modal frequency and first modal damping ratio are more sensitive to the damper at the top of the buildings than the others. The very small sensitivities to the dampers near the bottom of the buildings may indicate no need to install these dampers. The negative sensitivity, or gradient of the first modal damping ratio to damper stiffness is because as the damper stiffness increases the first modal damping ratio

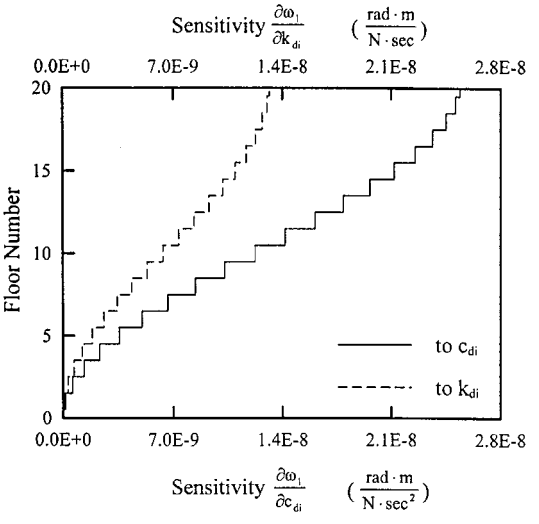

(a) Sensitivity of Modal Frequency

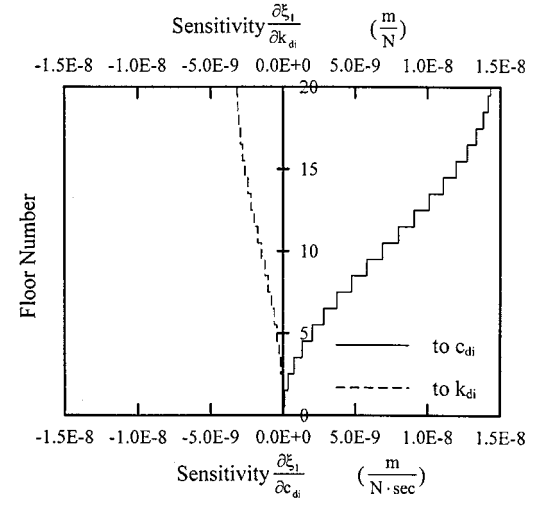

(b) Sensitivity of Modal Damping Ratio

Figure. 6. Sensitivities of modal frequency and modal damping ratio

decreases. Similar sensitivity results are found for the second modal frequency and damping ratio. Since all the sensitivity values are small even for the damper at the top of the buildings, one may conclude that the small deviations of the dampers from its optimal values ($c_d = 1 \times 10^6$ Ns/m and $k_d = 1 \times 10^5$ N/m) may not affect the control efficiency.

Seismic response

Seismic response analysis is carried out to investigate variations of seismic response of the adjacent buildings with damper parameters to see if the optimal damper parameters identified from the modal analysis are the same as those from the seismic response analysis under the given earthquake excitation spectrum. Then, the effectiveness of the dampers of optimal parameters on seismic response reduction is examined. Because of the limitation of space, only a few typical figures are given in this paper.

Figures 7 and 8 depict the variations of the top floor displacement responses of the left building and the right building, respectively, with damper stiffness for several damper damping coefficients. It is seen that the top floor displacement responses of both the left and right buildings are not affected by the damper stiffness if the damper stiffness is less than 1×10^5 N/m. The fact that the response mitigation is not sensitive to damper stiffness within a certain range is very helpful

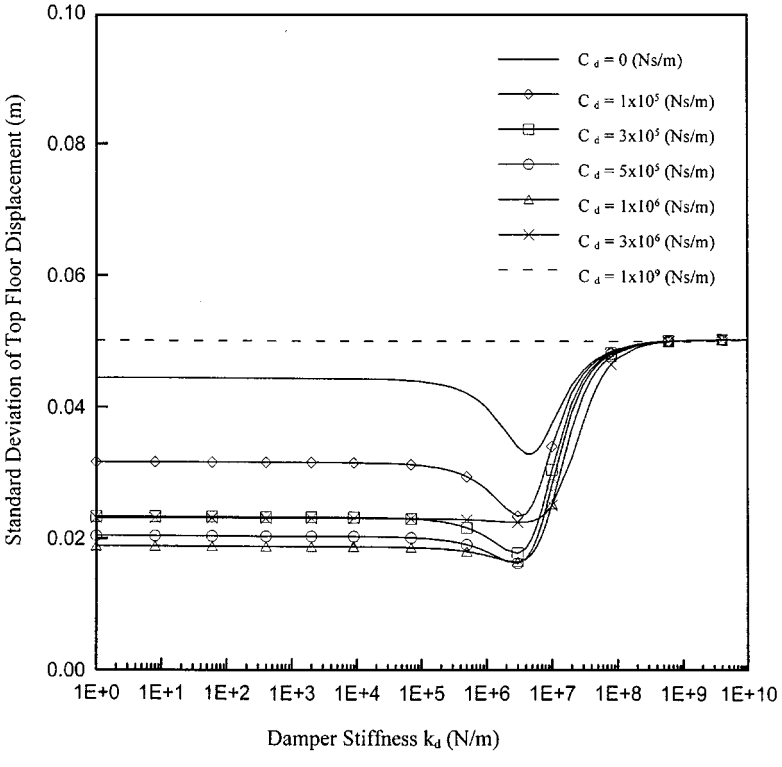

Figure. 7. Top floor displacement response of left building vs. damper stiffness

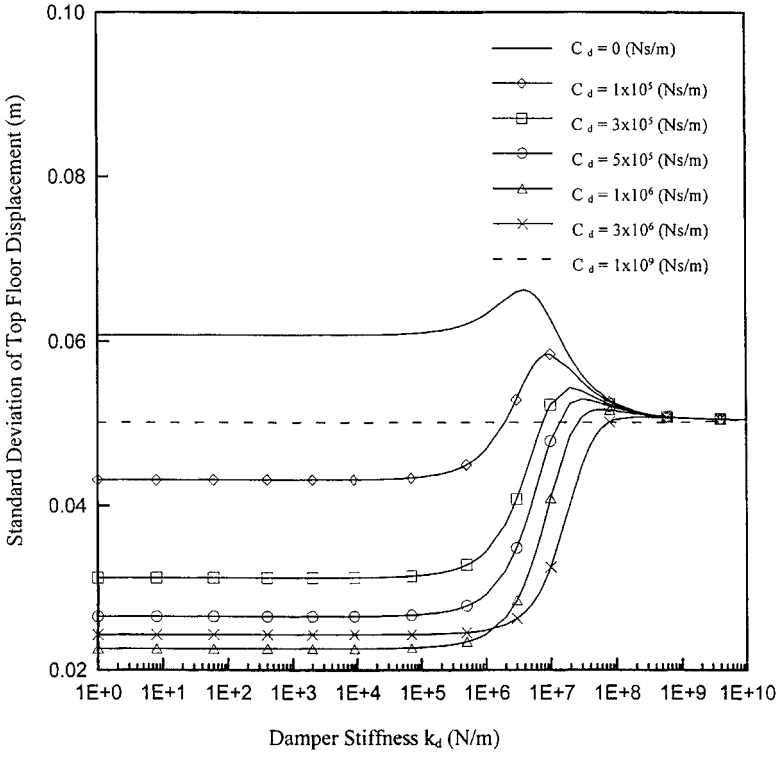

Figure. 8. Top floor displacement response of right building vs. damper stiffness

for the practical application of joint dampers. The further increase of the damper stiffness from 1×10^5 N/m may reduce the seismic response of the left building as shown in Figure 7, but it may increase the seismic response of the right building as shown in Figure 8. If the damper stiffness is increased to a level larger than 6×10^6 N/m, the effectiveness of joint dampers deteriorates rapidly. This is because the strong damper stiffness reduces the relative velocity of the damper and hence the energy absorbing capacity from the dampers decreases. In particular, when the damper stiffness reaches a value above 1×10^9 N/m, the relative displacement and velocity between the adjacent buildings become nearly zero so that the two buildings behave as though almost rigidly connected. As a result, no matter what value the damper damping coefficient is, the damper totally loses its effectiveness. It is clear from the foregoing two figures that to achieve the maximum reduction of the dynamic response of both buildings, the optimum damper stiffness should be less than 1×10^5 N/m, which is the same as the one found from the modal analysis. In addition, it can be seen from Figures 7 and 8 that there is an optimal damper damping coefficient between 5×10^5 and 3×10^6 Ns/m.

To find the optimal damper damping coefficient, the seismic responses including the top floor displacement response, the base shear force response, and the top floor acceleration response of both buildings are computed over a wide range of damper damping coefficient with an optimum damper stiffness being 1×10^5 N/m. Figure 9 shows the variations of the top floor displacement responses of the two buildings with damper damping coefficient. Clearly, the optimum damper

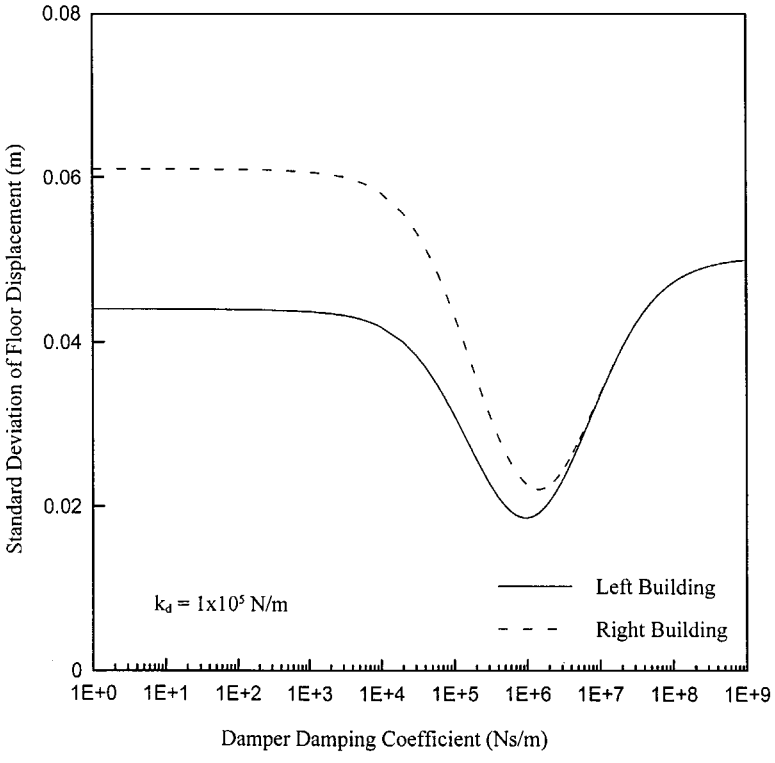

Figure. 9. Top floor dispolacement response of adjacent buildings vs. damper damping coefficient

damping coefficient is about 1×10^6 Ns/m at which the displacement responses of both buildings are reduced to the minimum. With the decrease of damping coefficient from the optimum value, the performance of the damper deteriorates gradually and as the damping coefficient approaches to zero the two buildings finally return to the unlinked situation. On the other hand, if the damping coefficient increases from the optimum value, the performance of the damper also declines and as the damping coefficient becomes very large the two buildings behave as though almost rigidly connected. As a result, the top floor displacements of the two buildings become the same. Again, the optimal value of damper damping coefficient found here is the same as the one found in the modal analysis.

The reason why the optimum values obtained from the modal analysis and seismic response analysis are the same is that the seismic displacement and shear force responses of both buildings are dominated by the first two modes of the system only (i.e. the first mode of the softer building plus the first mode of the stiffer building). Since the higher modes of vibration may have effects on the acceleration responses of both buildings, the optimum value of the damper damping coefficient found based on the acceleration response is a little larger than 10^6 Ns/m.

To demonstrate the overall effectiveness of the joint dampers, the standard deviations of displacement, shear force and acceleration responses at each floor for each building with and without joint dampers are computed using the Kanai–Tajimi excitation spectrum. Figure 10

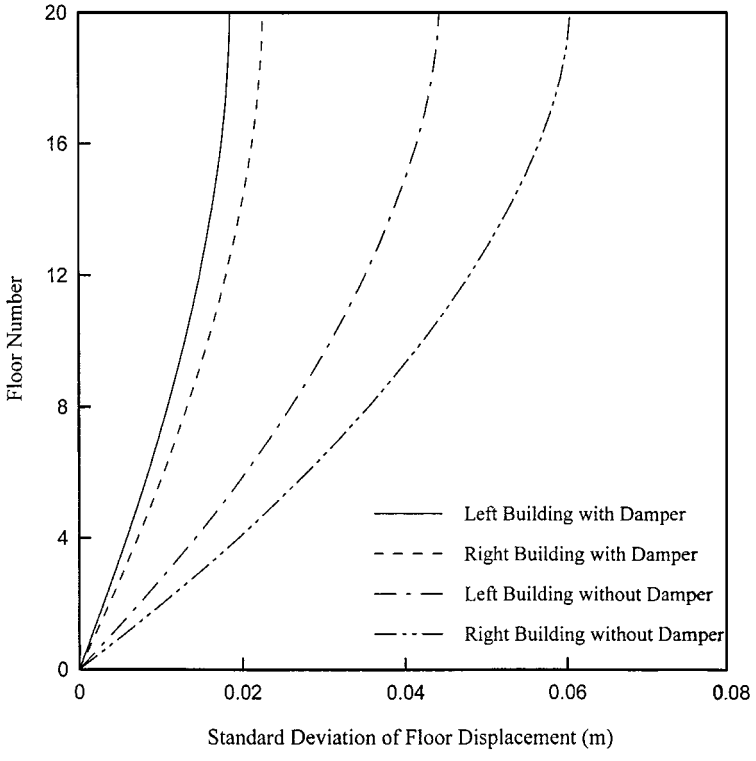

Figure. 10. Variations of diaplacement response of adjacent buildings with height

shows the variations of the standard deviation of displacement response relative to the ground with the height of the buildings. The top floor displacement standard deviation of the unlinked left building is 44·5 mm but with the joint dampers installed, it is reduced to 18·7 mm, leading to a 58 per cent reduction of the response. For right building, the top floor displacement standard deviation is 60·8 mm for the unlinked building and 22·7 mm for the linked building, resulting in a 63 per cent reduction. The reduction of the displacement responses from the joint dampers is also significant for other floors in either building. The standard deviations of shear force in each storey for each building are plotted in Figure 11. Unlike the adjacent building connected by hinged rigid links,[12] the shear forces in all the stories of both buildings are reduced after installation of the joint dampers. In particular, without the joint dampers the bottom shear force standard deviation is $1{\cdot}48 \times 10^7$ N in the left building and $1{\cdot}03 \times 10^7$ N in the right building. With the optimum joint dampers, the base shear force standard deviation is reduced to $5{\cdot}96 \times 10^6$ N in the left building and $3{\cdot}71 \times 10^6$ N in the right building, leading to a 60 and a 64 per cent reduction, respectively.

The variations of acceleration response with the building height, as shown in Figure 12, are different from the displacement and shear force response profiles shown in Figures 10 and 11. The acceleration response for each unlinked building does not vary monotonically with the height of the building. This is due to the contributions from higher modes of vibration.[4] Clearly, the joint

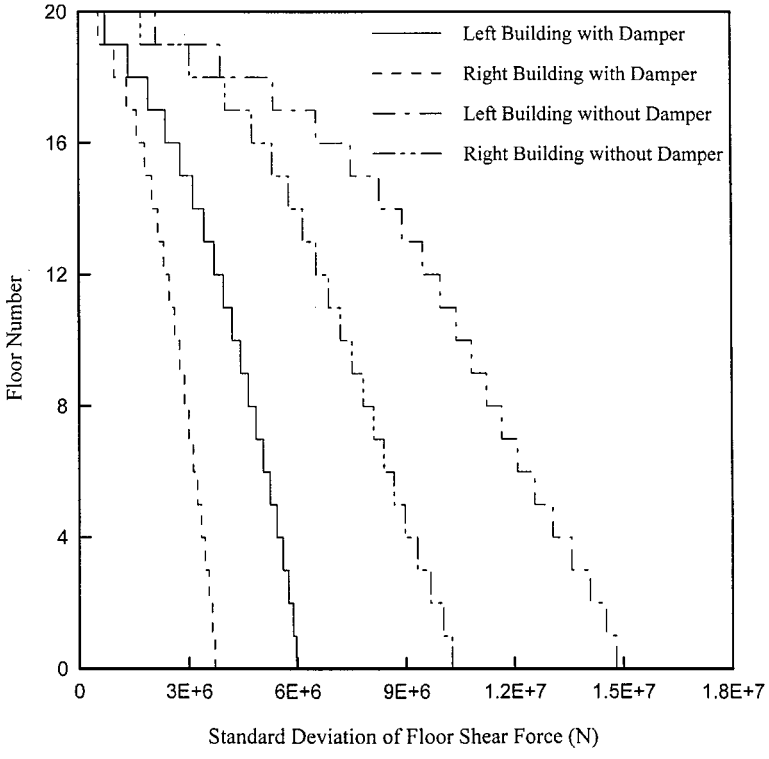

Figure. 11. Variations of shear force response of adjacent buildings with height

dampers effectively mitigate the acceleration responses not only from the low modes of vibration but also higher modes of vibration, as indicated by the response curves of the linked adjacent buildings.

CONCLUSIONS

An analytical method combining the complex mode superposition method with the pseudo-excitation method has been proposed in this paper for investigating both dynamic characteristics and seismic response of adjacent building connected by viscoelastic dampers. The method is mathematically accurate and computationally efficient. Based on the studies on the example adjacent buildings, it was found that if damper parameters are selected appropriately, the modal frequencies of the unlinked buildings could be retained and the modal damping ratios of the system could be significantly increased and thus the earthquake-induced dynamic responses of both buildings could be considerably reduced. The optimal values of the dampers found from the modal analysis with the maximum modal damping ratios as an objective were almost the same as those determined from the seismic response analysis with the maximum seismic response reduction as an objective. Some other issues related to this study, such as the optimal position of

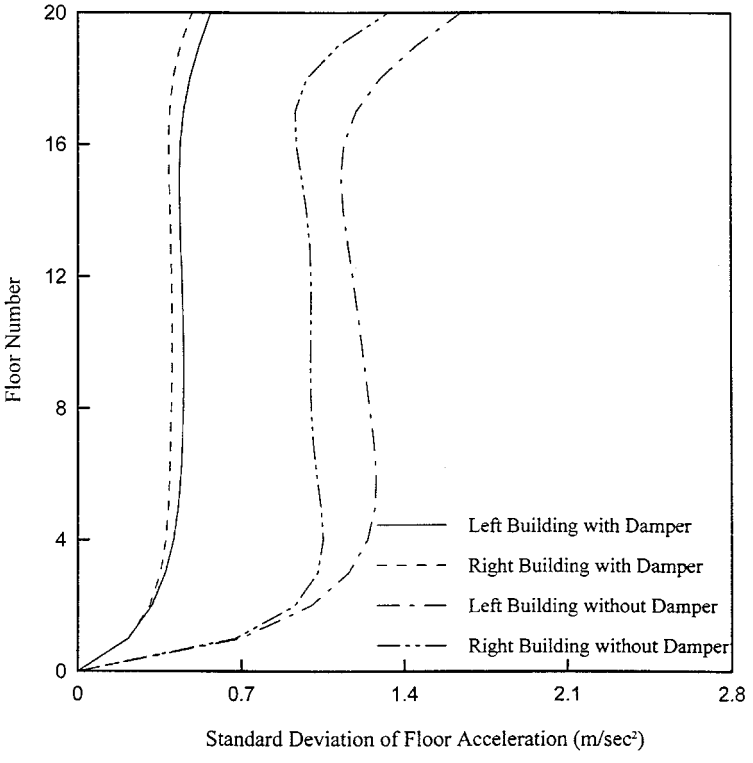

Figure. 12. Variations of acceleration response of adjacent buildings with height

dampers, the use of fluid dampers described by the Maxwell model, and the three-dimensional vibration mitigation analysis including torsional effects need further investigations.

ACKNOWLEDGEMENTS

The writers are grateful for the financial support from the Hong Kong Polytechnic University through a HKPU scholarship for the first author and its Area Strategic Development Program.

REFERENCES

1. T. Kobori, T. Yamada, Y. Takenaka, Y. Maeda and I. Nishimura, 'Effect of dynamic tuned connector on reduction of seismic response-application to adjacent office buildings', *Proc. 9th World Conf. on Earthquake Engineering*, Tokyo-Kyoto, Japan, Vol. V, pp. 773–778 (1988).
2. K. Seto and Y. Matsumoto, 'A structural vibration control method of flexible buildings in response to large earthquakes and strong winds', *Proc. 2nd Int. Workshop on Struct. Control*, Hong Kong, pp. 490–496 (1996).
3. Y. Yamada, N. Ikawa, H. Yokoyama and E. Tachibana, 'Active control of structures using the joint member with negative stiffness', *Proc. 1st World Conf. on Struct. Control.*, Los Angeles, California, U.S.A., Vol. 2, TP2, pp. 41–49 (1994).
4. Y. L. Xu, Q. He and J. M. Ko, 'Dynamic response of damper-connected adjacent buildings under earthquake excitation', *Engng. Struct.*, **21**, 135–148 (1999).
5. C. T. Sun and Y. P. Lu, '*Vibration Damping of Structural Elements*', Prentice-Hall, Englewood Cliffs, NJ, 1995.

6. M. P. Singh, 'Seismic response by SRSS for nonproportional damping', *J. Engng. Mech.* ASCE, **106**, 1405–1419 (1980).
7. T. Igusa, A. D. Kiureghian and J. L. Sackman, 'Modal decomposition method for stationary response of non-classically damper systems', *Earthquake Engng. Struct. Dyn.* **12**, 121–136 (1984).
8. S. Veletsos and C. E. Ventura, 'Modal analysis of non-classically damped linear systems', *Earthquake Engng. Struct. Dyn.* **14**, 217–243 (1986).
9. Claret and Venancio, 'A modal superposition pseudo-force method for dynamic analysis of structural systems with non-proportional damping', *Earthquake Engng. Struct. Dyn.* **20**, 303–315 (1991).
10. W. C. Hurty and M. F. Rubinstein, '*Dynamics of Structures*', Prentice-Hall, Englewood Cliffs, NJ, 1964.
11. J. H. Lin, W. S. Zhang and J. J. Li, 'Structural response to arbitrarily conherent stationary random excitations', *Comput. Struct.* **50**, 629–633 (1994).
12. B. Westermo, 'The dynamics of interstructural connection to prevent pounding', *Earthquake Engng. Struct. Dyn.* **18**, 687–699 (1989).

